K-Series X-Rays from π-Mesonic Atoms*†

M. CAMAC, A. D. MCGUIRE,‡ J. B. PLATT, AND H. J. SCHULTE§
University of Rochester, Rochester, New York

(Received April 28, 1955)

The K-series x-rays from the π-mesonic Be, B, C, N, and O atoms have been studied. In each case measurements have been made of the $2p$-$1s$ quantum energy, and of the fraction of stopped pions which give rise to K-series x-rays (the "K-series yield"). The yields are: Be, 18.8±1.7%; B, 13.6±1.5%; C, 9.5±1.0%; N, 4.5±0.5%; O, 3.4±0.4%. The decrease in yield with increasing Z is attributed to nuclear absorption of the pion from the $2p$ state. The $2p$-$1s$ quantum energies are: Be, 43±3.5 kev; B, 68±3.5 kev; C, 92±7.5 kev; N, 132±2.5 kev; O, 163.8±2.7 kev. The expected energy in the case of oxygen, if only electromagnetic interactions are important, is 176.0 kev; the difference is presumably due to a pion-nucleus interaction which is repulsive in the $1s$ state.

I. INTRODUCTION

THE formation of a mesonic atom as a step in the absorption process for negative mesons has been postulated for some time, and evidence for the existence of such atoms has been obtained both with cosmic ray[1–3] and machine produced[4–6] mesons. We have observed the K-series x-rays from the π-mesonic Be, B, C, N, and O atoms. In each case we have measured the quantum energy, and have determined the fraction of the stopped pions which give rise to radiative transitions to the mesonic $2s$ level.

The sequence of events from the stopping of a negative meson in condensed matter to the absorption of the meson by a nucleus has been considered in detail by several authors.[7] A pion is first bound to a particular nucleus in a quantum state characterized by large values of the principal and orbital quantum numbers ($n, l \sim 16$). The cascade process to lower energy states can occur through Auger[8] or radiative[9] transitions. The Auger effect predominates, in the low-Z elements considered here, for transitions between states of $n \geq 3$. Then radiative transitions become important, and nuclear capture competes with radiation in depleting these states of low quantum number.

Our determination of the fraction of stopped pions which give rise to the $2p$-$1s$ radiative transition (the $2p$-$1s$ "quantum yield") thus measures the nuclear capture probability for pions in the $2p$ state. We shall discuss the limits of validity of this measurement below. The branching ratio is expected to have a Z^2 dependence, since the radiative transition probability varies as Z^4 and the nuclear absorption probability varies as Z^6. (There are Z protons in the nucleus and the fraction of the time the $2p$ pion spends in the nucleus varies as Z^5.) Messiah and Marshak[10] predict the branching ratio to be $0.2Z^2$, and our results are consistent with this prediction.

The measured quantum energies are in all cases within 10% of the energies predicted by assuming electromagnetic interactions only between the pion and the nucleus. For nitrogen and oxygen, however, the measured $K\alpha$ quantum energies are less than the predicted values by 2% and 7% respectively. We believe these differences are significant. They pre-

* This research was assisted by the U. S. Atomic Energy Commission.

† Based in part on theses submitted by A.D. McGuire and H. J. Schulte to the Graduate School of the University of Rochester in partial fulfillment of the requirements for the degree of Doctor of Philosophy.

‡ Now at the University of Minnesota, Minneapolis, Minnesota.
§ Now at Los Alamos Scientific Laboratory, Los Alamos, New Mexico.

[1] Experimental evidence for radiative transitions in μ-mesonic atoms: W. Y. Chang, Revs. Modern Phys. **21**, 166 (1949); E. P. Hincks, Phys. Rev. **81**, 313 (1951); A. Farfarman and M. H. Shamos, Phys. Rev. **87**, 219 (1952); G. G. Harris and T. J. B. Shanley, Phys. Rev. **89**, 983 (1953); F. D. S. Butement, Phil. Mag. **44**, 208 (1953); W. Y. Chang, Phys. Rev. **95**, 1288 (1954).

[2] Experimental evidence for μ-mesonic Auger transitions: Cosyns, Dilworth, Occhialini, and Schoenberg, Proc. Phys. Soc. (London) **A62**, 801 (1949); C. Franzinetti, Phil. Mag. **41**, 86 (1950); W. F. Fry, Phys. Rev. **79**, 893 (1950); A. Bonetti and G. Tomasini, Nuovo cimento **8**, 693 (1951); Groetzinger, Leder, and Ribe, Phys. Rev. **81**, 626 (1951).

[3] Experimental evidence for π-mesonic Auger transitions: Menon, Muirhead, and Rochat, Phil. Mag. **41**, 583 (1950).

[4] Experimental evidence for radiative transitions in π-mesonic atoms: Camac, McGuire, Platt, and Schulte, Phys. Rev. **88**, 134 (1952); Schulte, Platt, and Camac, Phys. Rev. **89**, 905 (1953); Camac, Platt, and Schulte, Phys. Rev. **89**, 905 (1953); Stearns, DeBenedetti, Stearns, and Leipuner, Phys. Rev. **93**, 1123 (1954); McGuire, Camac, Halbert, and Platt, Phys. Rev. **95**, 625 (1954); Sterns, Sterns, Leipuner, and DeBenedetti, Phys. Rev. **95**, 625 (1954); Sterns, Sterns, DeBenedetti, and Leipuner, Phys. Rev. **95**, 1353 (1954); Sterns, Sterns, DeBenedetti, and Leipuner, Phys. Rev. **96**, 804 (1954); Sterns, Sterns, DeBenedetti, and Leipuner, Phys. Rev. **97**, 240 (1955).

[5] Experimental evidence for radiative transitions in μ-mesonic atoms: V. Fitch and J. Rainwater, Phys. Rev. **92**, 789 (1953); Sterns, DeBenedetti, Sterns, and Leipuner, Phys. Rev. **93**, 1123 (1954); Koslov, Fitch, and Rainwater, Phys. Rev. **95**, 291 (1954); **95**, 625 (1954).

[6] Experimental evidence for μ-mesonic Auger transitions: H. Morinaga and W. F. Fry, Nuovo cimento **10**, 308 (1953); W. F. Fry, Nuovo cimento **10**, 490 (1953).

[7] R. E. Marshak, *Meson Physics* (McGraw-Hill Book Company, Inc., New York, 1952), Chap. 5. Marshak gives a summary of the original papers and many references. References on the problem of meson capture not listed by Marshak include: R. Huby, Phil. Mag. **40**, 685 (1949); R. L. Rosenberg, Phil. Mag. **40**, 759 (1949).

[8] E. H. S. Burhop, *The Auger Effect* (Cambridge University Press, Cambridge, 1952), Chap. 7. G. R. Burbridge and A. H. de Borde, Phys. Rev. **89**, 189 (1953); B. L. Joffe and I. Ya. Pomeranchuk, Zhur. Eksptl. Teort. Fiz. **23**, No. 1 (7), 123-4 (1952); A. H. de Borde, Proc. Phys. Soc. (London) **A67**, 57 (1954).

[9] H. A. Bethe, *Handbuch der Physik* (Verlag Julius Springer, Berlin, 1933), second edition, Vol. **24**, Part 1, 440.

[10] A. M. L. Messiah and R. E. Marshak, Phys. Rev. **88**, 678 (1952).

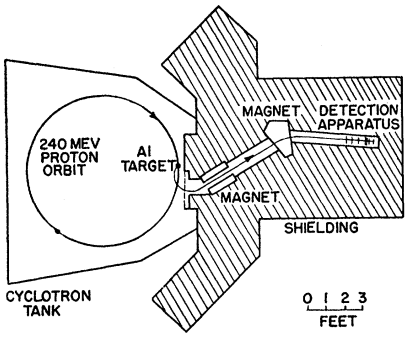

FIG. 1. Experimental arrangement in cyclotron room.

sumably indicate a meson-nuclear interaction which is repulsive for a meson in the $1s$ state.[11]

II. EXPERIMENTAL METHOD

The experiment arrangement is shown in Fig. 1. Pions were produced in an aluminum target in the University of Rochester 240-Mev synchrocyclotron. Negative pions of approximately 50-Mev energy were deflected and focused by the fringing field of the cyclotron magnet and by a separate external magnet. The π-meson beam was defined by the 6-in. horizontal and 3-in. vertical entrance aperture of the secondary magnet and by the $1\frac{1}{2}$-in. diameter of the meson telescope. Identification of the particles as pions was by their magnetic rigidity and range in aluminum.

X-Ray Detection Apparatus

The detection apparatus is shown schematically in Fig. 2. All detectors, except counter 5 were plastic scintillators. This apparatus was used both (1) for taking range measurements and determining the particle composition of the meson beam, and (2) for observing mesonic x-rays. A threefold telescope (counters 1, 2, and 3) defined the incoming pion beam. An aluminum step wedge between counters 2 and 3 was adjusted so that the pions stopped in a block of low-Z material inserted between counters 3 and 4. (We shall call the block the "stopper".) Counters 4 and 6 were used in anticoincidence. Counter 4 rejected events in which

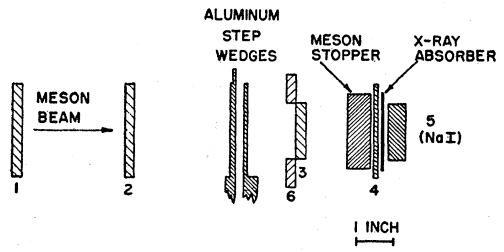

FIG. 2. Detection apparatus.

[11] Deser, Goldberger, Baumann, and Thirring, Phys. Rev. **96**, 774 (1954).

charged particles went completely through the meson stopper. Counter 6 was a 3 in.×3 in. plastic counter with a 1.5-in. diameter hole in the center. It rejected events in which a pion outside the beam defined by counter 3 gave rise to a count in 3 by a secondary process.

The x-ray detector, counter 5, was a cylindrical NaI(Tl) crystal of $1\frac{1}{2}$ in. diameter enclosed in a moisture-proof container[12] and mounted on the photocathode of a DuMont type 7292 photomultiplier. Its thickness was equal to several mean free paths for the x-rays under study.

A block diagram of the coincidence circuit is shown in Fig. 3. The resolving time of the coincidence system

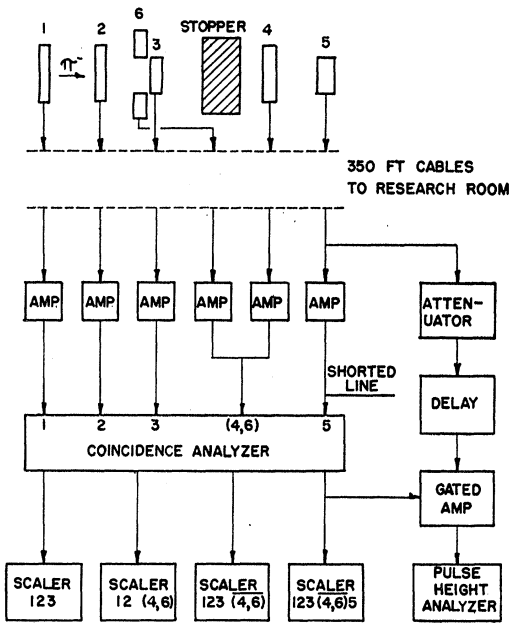

FIG. 3. Simplified block diagram of the electronic equipment. Coincidence inputs to scalers shown here are those used while recording mesonic x-ray spectra. Other coincidence combinations could be selected for other purposes.

was about 5×10^{-8} sec. Events causing the coincidence, anticoincidence combination $1\text{–}2\text{–}3\text{–}\bar{4}\text{–}5\text{–}\bar{6}$ opened the 0.5-microsecond gate of the gated amplifier. The amplitude spectrum of the pulses in counter 5 which occurred in time coincidence with the above type of event was measured on the 24-channel pulse-height analyzer. Energy calibration of the system was established by means of x-rays from artificial radioactive sources.

Because of the large amount of background radiation and the high detection efficiency of the NaI crystal, approximately five feet of brass were required as shielding between the cyclotron and the x-ray detector. The purpose of the shielding was to attenuate fast particles (mainly neutrons) originating in the cyclotron.

[12] C. J. Borkowski and R. L. Clark, Rev. Sci. Instr. **24**, 1046 (1953).

In addition the detector was surrounded in all directions except that of the incident pion beam, by several additional feet of brass, lead, and concrete to attenuate secondary neutrons and gamma rays which scattered about the cyclotron building. Under operating conditions, a typical background counting rate of events in which more than 20 kev of energy was lost to the NaI crystal was 3×10^4/sec during the time the proton beam irradiated the target. At such background counting rates the random coincidence rate of 1–2–3–$\bar{4}$–5 events (the bar denotes anticoincidence) was negligible, and the probability of detecting an unwanted event in an arbitrary opening of the 0.5-μsec gate was also negligible ($\sim10^{-3}$). We nevertheless observed broadening of the x-ray pulse height spectra if the background substantially exceeded this value. We believe the important time constant in this connection is the recovery time of the NaI crystal from the occurrence of a high-energy event to the time at which this event contributes a negligible fluctuation ($\ll$20 kev) from the average light output from the crystal.

Range Measurements

Integral range curves were taken by plotting the number of coincidence events 1–2–3–4 as a function of the thickness of aluminum between counters 2 and 3, using the number of 1–2 coincidence events as a monitor. The thickness of aluminum was varied in steps of $\frac{1}{2}$ g/cm^2. This procedure then yields the number of incident particles which penetrate the entire length of the telescope. An integral range curve and its derivative are shown in Fig. 4. The mean range corresponds to an initial energy of 51.5 Mev. The width of the derivative is consistent with a spread in the incident energy of about 1 Mev.

Differential range curves were obtained by plotting the combination 1–2–3–$\bar{4}$ *versus* aluminum thickness, again using 1–2 coincidence events as the monitor. An event 1–2–3–$\bar{4}$ represents a meson stopping in either the stopper or counter 3. Figure 5 shows typical differential range curves taken with and without the meson stopper in place. The peak in the lower curve of Fig. 5, taken with the stopper removed, represents particles stopping in counter 3. The ordinate of the stopper in-out difference curve represents particles stopping in the stopper only; the width indicates the thickness of the stopper in equivalent range in aluminum.

The beam contamination consists primarily of muons and electrons that originate in the vicinity of the target and have the acceptable magnetic rigidity. A determination of the range of the particles of identical magnetic rigidity should suffice to identify the components of the beam. For 51.5-Mev pions, muons of the same momentum should have 62-Mev energy and a a range of 18 g/cm^2 of Al; electrons should have 130-Mev energy and a range of over 20 g/cm^2 of Al. In addition, some pions undergo decay in flight after

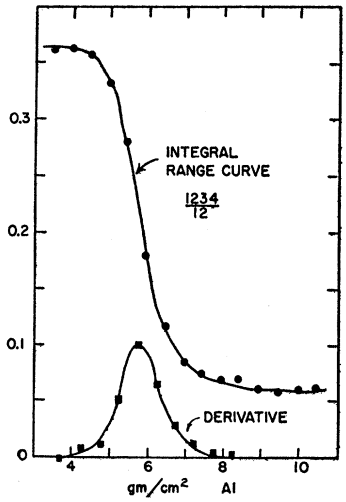

FIG. 4. Typical integral range curve and its derivative, taken with meson stopper in place.

magnetic analysis. The decay muons whose paths are parallel or antiparallel to the pion trajectory also may contaminate the beam. Each of these components has been identified in range measurements and checked by specific ionization measurements in a thin NaI crystal.

In addition to the above contamination of the pion beam, we have also found x-ray evidence for muons with the same range as the pions. In the experiments reported here, these muons are mainly due to $\pi-\mu$ decays in the counter telescope after the pions lose most of their energy. Calculations show that roughly 0.5% of the pions should undergo such decay. Muons with the same range as 51-Mev pions may also arise from pions of lower energy that decay in the fringing field of the cyclotron. These muons enter the secondary

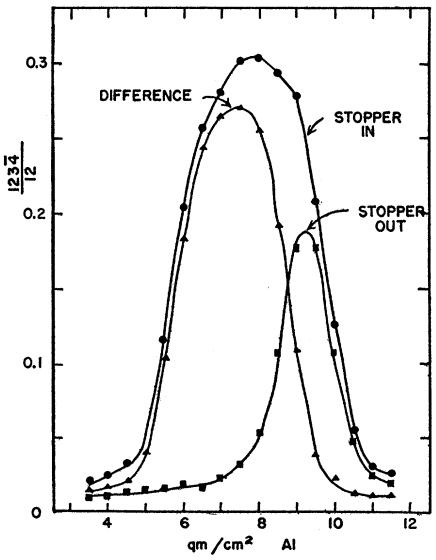

FIG. 5. Typical differential range curves taken with and without the meson stopper in place. The difference between the two is also shown.

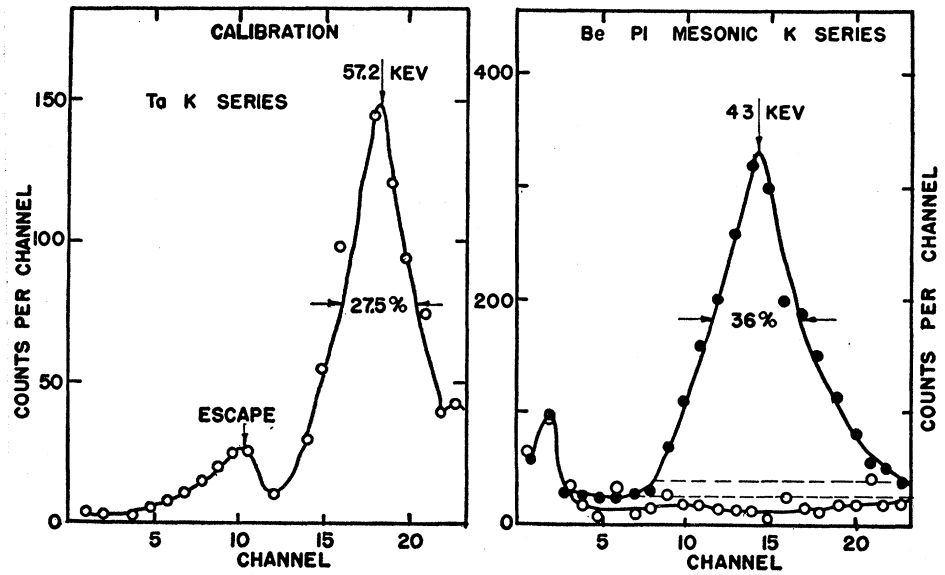

FIG. 6. Beryllium K-series π-mesonic x-ray spectrum and tantalum K-fluorescence calibration spectrum. The lower curve of the Be data was taken with a 0.022-in. Pb absorber in front of the x-ray detector.

magnet at different angles than the pions but a fraction may still be focused in the detection apparatus.

Since the μ-mesonic x-ray yield is large, compared to a π-mesonic x-ray yield of a few percent for oxygen, the μ-mesonic x-rays serve as a sensitive indication of the μ contamination of the stopping particles. The fraction of the stopped particles which give rise to μ-mesonic x-rays, assuming a 100% yield for muons, is measured to be about 1% (see Fig. 9). In work reported earlier,[13] the energy resolution of the NaI scintillation spectrometer was not sufficient to separate the π and μ contribution and no correction was made to the data for the μ contamination of the beam of the correct range. We now believe that our previously published oxygen yield was substantially in error for this reason.

III. MESONIC X-RAY MEASUREMENTS

The materials used as meson stoppers were beryllium metal, boron metal, carbon (graphite or CH_2), hydrazine (N_2H_4) and water. The stoppers were all of nearly the same thickness as that indicated in the differential range curve of Fig. 5; i.e., approximately 2.5 g/cm^2.

The response of the x-ray detector to monoenergetic x-rays was determined with x-rays from artifically radioactive sources. A low-intensity Hg^{203} source[14] was deposited permanently on counter 4. Both the 279-kev nuclear γ ray[15] following β decay of Hg^{203} and the 72.1-K x-rays of Tl (following internal conversion) were observed in the x-ray counter in coincidence with β pulses in counter 4. Calibration curves were taken during the meson runs with the equipment in all respects in the same condition as when mesonic x-rays were being observed, except that the cyclotron was turned off, and the gated amplifier was triggered with β rather than meson events.

Identification of the observed radiation as mesonic x-rays rests on the following: The pulse-height spectrum of pulses in the x-ray detector in coincidence with mesons stopping in the stopper displayed a maximum in each case within 10% of the energy predicted for the mesonic K x-ray for the element of the stopper. By introduction of metal foils between the meson stopper and the detector, it was established that the peaks in the spectra yielded the expected[16] x-ray absorption curves. Such a foil is shown in Fig. 2 as "x-ray absorber."

Beryllium

Figure 6 shows the pulse-height spectrum of pulses in counter 5 in coincidence with π^- mesons stopping in beryllium. The callibration curve of Fig. 6 was obtained during the beryllium runs the same amplifier gain, so that the abscissae of the two curves are identical. The zero of energy is in channel 1. The calibration curve is that of the fluorescent radiation from Ta emitted when x-rays from the Hg^{203} source were absorbed in a thin Ta foil placed in the "x-ray absorber" position (Fig. 2). The familiar escape peak[17] is seen in the calibration curve.

The predicted instrumental width for the spectrum of a monochromatic x-ray line at the π-mesonic Be $K\alpha$ energy, extrapolating the observed width at the calibration energy by use of an $E^{-\frac{1}{2}}$ energy dependence, is 31%. The observed width is 36% The discrepancy may be

[13] Camac, McGuire, Platt, and Schulte, Phys. Rev. **88**, 134 (1952); Camac, Platt, and Schulte, Phys. Rev. **89**, 905 (1953).
[14] Purchased from Oak Ridge National Laboratory.
[15] Hollander, Perlman, and Seaborg, Revs. Modern Phys. **25**, 469 (1953).
[16] A. H. Compton and S. K. Allison, *X-Rays in Theory and Experiment* (D. Van Nostrand Company, Inc., New York, 1935), Appendix 9.
[17] P. Axel, Rev. Sci. Instr. **25**, 391 (1954).

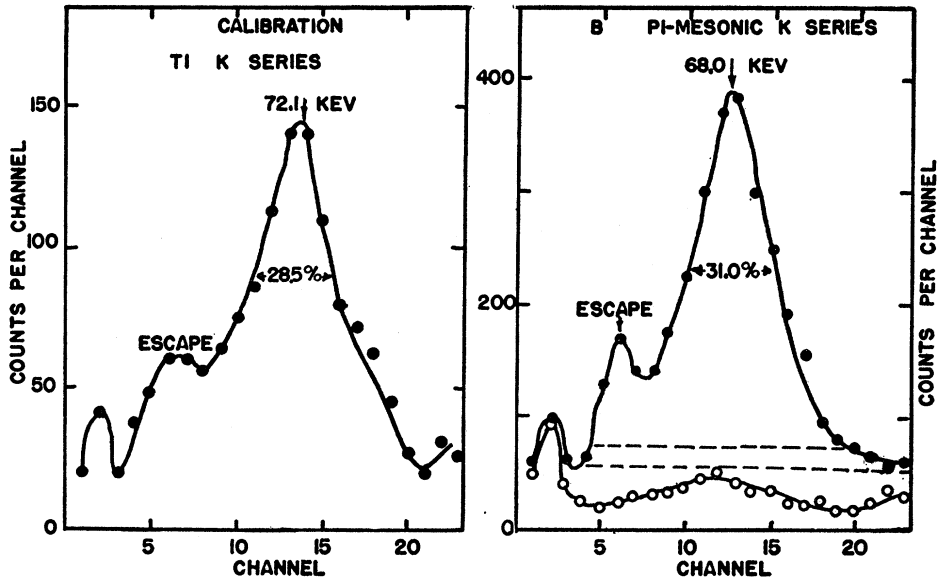

FIG. 7. Boron K-series π-mesonic x-ray spectrum and thallium K x-ray calibration spectrum. The lower curve of the B data was taken with a 0.050-in. W absorber in front of the x-ray detector.

due to the presence of x-rays from higher transitions, or Compton broadening by the stopper and background broadening. We adopt the interpretation that the observed Be π-mesonic x-ray spectrum consists of $K\alpha$ radiation with possible radiation from $K\beta$ and higher transitions, in unknown relative intensities. The measured energy of the peak of the Be spectrum is 43±3.5 kev. The weighted average energy of the Ta K calibration spectrum was taken to be 57.2 kev.

To aid in the determination of the background to be subtracted in determination of the mesonic x-ray yield, a run was made with a 0.022-in. thick Pb absorber in place for the same number of stopped mesons as in the upper curve. The true background must lie above the lower curve since the Pb absorber must remove some of the background in addition to absorbing the mesonic x-rays. The true background was assumed to lie between the dashed lines shown. Uncertainty in the knowledge of the background to be subtracted constitutes the dominant error in the yield measurement.

Boron

In the boron mesonic x-ray spectrum of Fig. 7 it was determined that the energy threshold of the amplifier gate was sufficiently low not to distort the shape of the escape peak associated with the boron mesonic x-rays. This procedure insures that all of the main peak was above threshold. The calibration for boron was established with the Tl K x-rays from the Hg^{203} source. The abscissas of the curves are identical, the zero of energy being in channel 4 in this case. In both curves, the escape peaks appear in the predicted channels. Using 72.1 kev as the energy of the peak in the calibration curve leads to a value of 68.0 kev for the peak of the boron mesonic x-ray curve.

The width of the boron mesonic x-ray curve predicted from the width of the calibration curve is 29.4%, while 31.0% is observed. This observed width is not consistent with an intensity of the π-mesonic $K\beta$ line of more than 25% of that of the $K\alpha$ even if no other source of line broadening were present. The interpretation adopted is that the $K\alpha$ line represents at least 75% of the intensity of the boron π-mesonic K series, and that the observed energy of the boron $\pi K\alpha$ line is 68±3.5 kev.

The lower curve of Fig. 7 was taken with a 0.050-in. thick tungsten absorber in order to estimate the background. Some evidence of tungsten fluorescence can be seen in the lower curve. The true background was assumed to lie between the two dashed lines shown.

Carbon

For carbon, no difference in mesonic x-ray yield was found from graphite and from CH_2 stoppers, which supports the assumption that hydrogen present in chemical combination plays a negligible role in the formation of the mesonic atom.[7] The spectrum (not shown) from carbon appears considerably broader than predicted from the calibration curves. The excess width of this spectrum is attributed to drift in gain of an amplifier during the taking of the data, and to a higher background counting rate in the x-ray detector. The cyclotron was intentionally operated at higher beam level than optimum for best resolution in order to speed the taking of data. Speculation as to the relative intensity of the $K\alpha$ and $K\beta$ lines in carbon on the basis of the observed line widths does not seem profitable. Within the experimental accuracy, the peak in the carbon mesonic x-ray spectrum appears at the energy predicted for the $K\alpha$ lines.

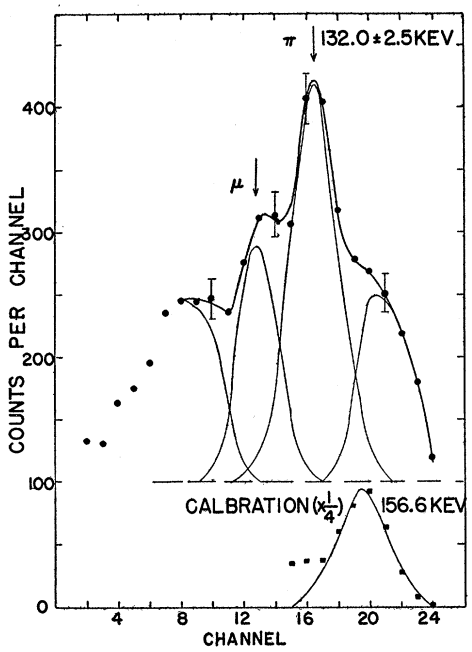

FIG. 8. Nitrogen K-series mesonic x-ray spectrum and calibration. The arrow marked π locates the center of the observed $K\alpha\pi$ x-ray peak. The one marked μ is placed at the predicted $\mu K\alpha$ x-ray energy. The dashed line indicates the background level assumed for the yield calculation. Zero energy is in channel zero.

Nitrogen

The pulse-height spectrum obtained for the nitrogen K-series mesonic x-rays is shown in Fig. 8. The background is much more prominent than with lower-Z elements, because the higher quantum energy requires a thicker NaI crystal and hence more sensitive volume for detection of stray radiation. In addition, the x-ray yield is less than for lower-Z elements.

The higher quantum energy (approximately 132 kev) permits increased resolution, and contributions are apparent from $3p$-$1s$ and higher radiative transitions. This component appears at an energy of approximately 163 kev. One also sees a component at 103 kev attributed to nitrogen μ-mesonic x-rays from the muon contamination in the beam. The observed spectrum was resolved into components of the same line shape as the calibration spectrum, and upper and lower limits on the background were again established with the aid of a thick absorber. We find that 80±5% of the π-mesonic K-series radiation appears in the $2p$-$1s$ line, and that $3p$-$1s$ and higher transitions account for the remaining 20±5%. None of the observed $3p$-$1s$ and higher transition intensity can be attributed to simultaneous collection of K- and L-series quanta, since 0.016 in. of copper foil was used to filter the x-rays. The μ-mesonic x-ray intensity is consistent with 1.5% muon contribution to the stopped particles, if one assumes that all muons give K x-rays.

The energy calibration was established with a Cd^{111} γ ray[15] taken to have an energy of 171.2 kev. Since this γ ray is followed by a delayed γ ray, it was convenient to delay the calibration signal for coincidence, and the delay line attenuated the calibration signal by a known amount to correspond to a quantum energy of 156.8±1.5 Kev. The width of the nitrogen mesonic $2p$-$1s$ line, predicted from calibration, is 23% of the peak energy. The observed spectrum resolves into a component of width 22±2%.

The energy of the nitrogen π-mesonic $K\alpha$ x-ray line is measured to be 132.2±2.5 kev.

Oxygen

The pulse-height spectrum resulting from pions stopping in water is shown in Fig. 9. Resolution into components has been done in the same manner as that described above for nitrogen, except that a small component at ~100 kev has been added. Such a component is expected from the mesonic carbon K x-rays, due to pions stopping in the last telescope crystal; one can estimate this contribution. The μ x-ray peak at 132 kev, and the peak due to $K\beta$ and higher transitions at 210 kev, are again evident. The full width at half-maximum of the observed $K\alpha$ line is 20±2%, in agreement with the calibration curve. The calibration was again established with the 171.2 kev Cd^{11} γ ray, attenuated to correspond to a quantum energy of 156.8±1.5 kev. In plotting the calibration spectrum of Fig. 9 a correction has been made for this attenuation. The energy of the O $K\alpha$ line is measured to be 163.8±2.7 kev. The relative intensities of the K-series radiations are $K\alpha$: 79%±9%; $K\beta$ and higher transitions: 21%±6%.

Determination of Yields

The fraction of stopped pions that yield K-series mesonic x-rays is plotted as a function of the atomic

TABLE I. Quantities used in calculation of K yields, and total K-series yields.

Element	Number of x-ray counts N_x	Number of stopped mesons N_π	Escape correction E	Scattering and absorption correction K	Efficiency-solid angle product ϵ	Total K-series yield Y
Be	1915±170	1.04×10^5	0.83	0.93	0.131	0.188±0.017
B	2535±270	1.47×10^5	1.00	1.07	0.111	0.136±0.015
C	1105±120	1.02×10^5	1.00	1.03	0.101	0.095±0.010
N	1420±150	2.95×10^5	1.00	0.97	0.112	0.045±0.005
O	3280±360	9.99×10^5	1.00	0.94	0.100	0.034±0.004

number of the stopper in Fig. 10. These yields were calculated from the formula

$$Y=\frac{N_x}{N_\pi \epsilon E K}-C_\mu,$$

where Y is the yield. The remaining symbols are defined and their determination from experimental data is discussed below. Table I lists the values of these quantities obtained in our experiments.

N_x is the number of observed x-rays, obtained by determining the total area under the appropriate peak in the pulse height spectrum, and subtracting the background assigned by the methods previously discussed. In all cases, uncertainty in the assignment of background is the dominant error. For Be, B, and C this summation includes both π- and μ-mesonic x-rays.

E is a correction required in the case of Be to take account of x-rays collected by the counter but undetected because of escape of the fluorescent iodine quantum. E is computed from the graph of Axel.[17] For the other elements the "escape peak" fell within the range of detection and the summation included these events.

C_μ is the contribution to the observed yield from μ-mesonic x-rays. This quantity was experimentally determined in the case of oxygen, where it is appreciable compared to the π-mesonic x-ray yield and where the two peaks can be resolved; C_μ in this case is 0.009. The same value was assumed to be appropriate for Be, B, and C. In the case of nitrogen the two peaks were resolved and this correction was not made.

N_π is the number of stopped pions. It is determined by counting the coincidence events 1–2–3–$\bar{4}$–6 and multiplying by the fraction of beam particles which come to rest in the stopper as determined from the differential range curves. This fraction was usually about 0.86.

ϵ is the probability that an x-ray quantum originating in the stopper would be detected by the counter if no matter intervened between the point of origin and the counter. ϵ was computed by determining the counter efficiency-solid angle product for a number of source points within the stopper, and then taking the weighted average of such results over the volume in which the mesons stopped. The details of this calculation are given elsewhere.[18]

K is the correction required for Compton scattering and photoelectric absorption of x-rays in the matter around the source point and the counter; that is, the meson stopper, anticoincidence counter 4, any metal foils used as x-ray filters, and the aluminum shell housing the NaI crystal. K was calculated from the known cross sections for absorption and scattering, using a mechanical model to perform the spatial integrations over differential scattering cross sections. This result was checked at quantum energies of 32 kev (Cs^{137}) and 72 kev (Hg^{203}) by measurement with an "analog". A point source of the radioisotope was placed in the desired source position with respect to the x-ray counter, and the relative counting rates were found with the source (1) bare, and (2) surrounded by material of the same electron density, shape and position relative to the counter as that used during mesonic x-ray runs. For both methods a number of source

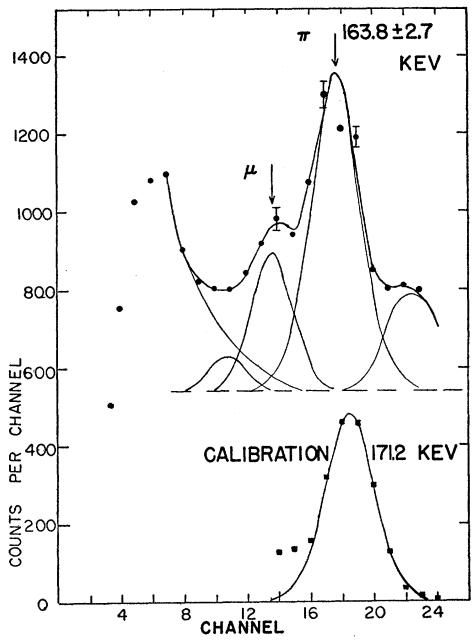

FIG. 9. Oxygen K-series mesonic x-ray spectrum and calibration. The arrow marked π locates the center of the observed $K\alpha\pi$ x-ray peak. The one marked μ is placed at the predicted $\mu K\alpha$ x-ray energy. The dashed line indicates the background level assumed for the yield calculation. The small peak near channel 11 is the expected contribution due to carbon π x-rays from mesons stopping in counter 3. Zero energy is in channel zero.

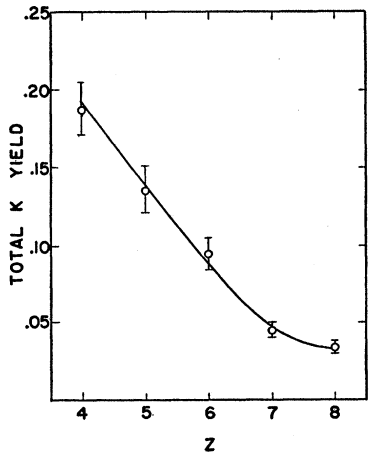

FIG. 10. Total K-series yield *vs* Z.

[18] A. D. McGuire, thesis, University of Rochester, 1954 (unpublished).

TABLE II. Data on radiative and absorption probabilities for pions in $2p$ state.

Element	$K\alpha$ yield $Y_{2p\text{-}1s}$	Population of $2p$ level P_{2p} Upper limit	Lower limit	Ratio of absorption to radiation probability W_a/W_r Upper	Lower	Predicted
Be	0.150±0.016	0.80±0.05		4.3±0.7		3.2
B	0.109±0.014	0.80±0.05		6.3±1.0		5.0
C	0.076±0.009	0.80±0.05	0.18±0.06	9.5±1.4	2.4±1.1	7.2
N	0.040±0.008	0.80±0.05	0.25±0.06	19±4	5.2±2.0	9.8
O	0.031±0.010	0.80±0.05	0.34±0.03	25±10	9.9±4.8	12.8

points were used, and K is the weighted average over the volume in which pions stopped. The two methods were in good agreement; we found by either method that the Compton scattering probability for a single quantum is about 20%, but in the aggregate, for our geometry, the in-scattering is nearly equal to the out-scattering plus absorption.

IV. CONCLUSIONS

Nuclear Absorption

The yields of the π-mesonic K-series x-rays furnish information on the pion absorption rate by the nucleus from the $2p$ state. Consider the $2p$-$1s$ mesonic x-ray. In order to emit this x-ray the pion must first reach the $2p$ level; let P_{2p} be the probability that a stopped pion reaches the $2p$ state. The pion then makes the radiative transition to the $1s$ state or else undergoes nuclear absorption from the $2p$ state; let the probability per second for these processes be W_r and W_a respectively. (The probability of an Auger transition or of π-μ decay is negligible.) Hence

$$Y_{2p\text{-}1s}=P_{2p}W_r/(W_a+W_r),$$

and

$$W_a=W_r\{(P_{2p}/Y_{2p\text{-}1s})-1\}.$$

Since the mesonic atom is hydrogen-like, W_r is readily evaluated: $W_r=1.75\times10^{11}Z^4$ sec^{-1}. $Y_{2p\text{-}1s}$ is measured directly in this experiment for nitrogen and oxygen, and for the other three elements it is reasonable to assume that the $2p$-$1s$ yield is 80% of the total K yield.

P_{2p} can only be bounded with our present information. Since 20% of the K-series radiation is observed to come from $3p$-$1s$ and higher transitions, P_{2p} cannot exceed 0.80. A lower limit can be obtained from the L-series yields given in the following paper,[19] at least in the cases of O, N, and C, since mesons yielding L-series radiation must occupy the $2p$ state (or the $2s$ state, but it is much more probable that a meson initially in a $3p$ or higher p state radiates to the $1s$ level). Table II lists the upper and lower limits obtained for the ratio W_a/W_r, together with the values of this quantity predicted by Messiah and Marshak.[10]

TABLE III. Observed and predicted $2p$-$1s$ quantum energies.

Element	Observed energy kev	Predicted from electromagnetic interactions kev	Energy difference Observed kev	Predicted by Deser *et al.* kev
Be	43 ±3.5	43.9	− 1 ±3.5	− 1.85
B	68 ±3.5	68.8	− 1 ±3.5	− 4.2
C	92 ±7.5	99.1	− 7 ±7.5	− 5.6
N	132 ±2.5	134.9	− 2.7±2.5	−10.4
O	163.8±2.7	176.0	−12.2±2.7	−17.7

Quantum Energies

The measured energies of the mesonic $K\alpha$ x-rays ($2p$-$1s$ transitions) are given in Table III for the five elements reported here. We list in the same table the predicted x-ray energies assuming electromagnetic effects only. These predicted values are found by solution of the Klein-Gordon equation for the hydrogenic (point nucleus) meson-nucleus system, and the use of these solutions in first-order perturbation calculations to find the corrections required for the finite extent of the nucleus and the polarization of the vacuum. These calculations have been performed by Grunstra and are described in detail elsewhere[20]; his methods are essentially similar to those used by the Columbia and the Carnegie groups.[21]

Differences between the observed and the predicted quantum energies are presumably due to a non-electromagnetic interaction between the pion and the nucleus. Such an effect is expected because of the pion-nucleon interaction. Estimates have recently been made by Deser, *et al.*[11] of the energy shift of the $1s$ level resulting from the pion-nucleon interaction. These estimates make use of the pion-nucleon scattering lengths given by Orear[22] and assume that the scattering lengths of the nucleons in the nucleus are additive.

We include in Table III a comparison of the observed energy shifts with those predicted by Deser *et al.* We find, as does the Carnegie group, some evidence for a nonelectromagnetic interaction.

[19] Camac, Halbert, and Platt, following paper [Phys. Rev. **99**, 905 (1955)].

[20] B. R. Grunstra, thesis, University of Rochester, 1954 (unpublished).

[21] Specifically, these calculations assume a pion mass of $272.7m_e$; the nucleus a sphere of uniform charge density and radius $1.2\times10^{-13}A^{\frac{1}{3}}$ cm; and no energy shift due to polarization of the nuclear charge. Grunstra estimates that this last effect, if present, does not change these quoted energies by more than 0.5%.

[22] J. Orear, Phys. Rev. **96**, 176 (1954).

ACKNOWLEDGMENTS

We are indebted to Dr. Messiah and Dr. Marshak for theoretical guidance, as we are to Dr. Kroll of Columbia University and to Professor Wentzel of Chicago. This research has been a group effort, and we are grateful to the members of our group, not primarily concerned with the work reported here, for many suggestions and much help. These men are Dr. M. L. Halbert and E. K. Gatchell, B. R. Grunstra, W. B. Johnson, P. P. Kane, and M. E. Nordberg, Jr.

PHYSICAL REVIEW VOLUME 99, NUMBER 3 AUGUST 1, 1955

L-Series X-Rays from π-Mesonic Atoms*†

M. CAMAC, M. L. HALBERT, AND J. B. PLATT
University of Rochester, Rochester, New York

(Received April 28, 1955)

The yields of the L-series x-ray lines from π-mesonic atoms have been measured for fourteen elements between $Z=6$ and 26. The total yield rises from 18% at carbon to a maximum of about 70% in the vicinity of aluminum, and then decreases. This decrease is caused primarily by nuclear absorption of pions from the $3d$ state; the $3d\rightarrow 2p$ yield determinations thus measure the nuclear absorption rate from the $3d$ state. The low-Z drop-off is predicted qualitatively by theoretical calculations of the meson cascade scheme. The observed relative intensities of the different L-series emission lines are substantially independent of Z in the range $6\leqq Z\leqq 16$. The $3d\rightarrow 2p$ transition energies are consistent with electromagnetically predicted values within the experimental error of 3 to 5% for $Z\leq 28$.

I. INTRODUCTION

THE x-ray emission lines from pi-mesonic atoms of light nuclei have been studied by Sterns, DeBenedetti, Stearns and Leipuner[1] and by Camac, McGuire, Platt, and Schulte.[2,3] Using the same equipment and similar techniques as the latter group we have measured the yield and the relative intensities of the L series for the elements $Z=6$ to 17 inclusive (except $Z=10$) and also $Z=20$, 22, and 26. These data furnish information on the competition between the $3d\rightarrow 2p$ radiative transition and the nuclear absorption of pions from the $3d$ state, and also on the cascade scheme of the mesonic atom. We have obtained energy measurements of the $3d\rightarrow 2p$ transitions for some of these elements, providing additional information on the specific pion-nucleus interaction.

The formation of the mesonic atom and details of the experimental procedure are described in the preceding article.[3] We proceed here with a discussion of the L-series data.

II. EXPERIMENTAL DATA

To illustrate the important features of the L-series data, we discuss in detail spectra obtained from several elements. We have chosen the spectra of oxygen, aluminum, and iron, shown in Figs. 1, 3, and 4. The vertical scales have been adjusted so that each spectrum is normalized to the same number of stopped mesons as the no-absorber spectrum for that element. The bars shown represent the standard deviation in a representative point.

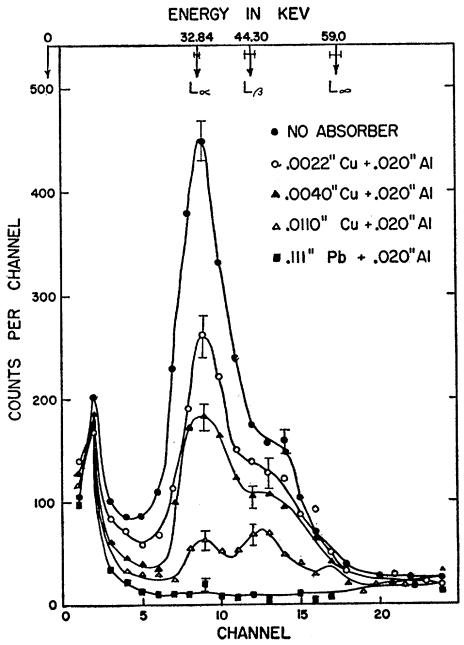

FIG. 1. Oxygen L series. Each spectrum was taken with the indicated x-ray absorber placed in front of the x-ray detector. The energy scale was determined by independent calibration with radioisotopes.

* This research was assisted by the U. S. Atomic Energy Commission.

† Based on a thesis submitted by M. L. Halbert to the Graduate School of the University of Rochester in partial fulfillment of the requirements for the degree of Doctor of Philosophy.

[1] Stearns, DeBenedetti, Stearns, and Leipuner, Phys. Rev. **93**, 1123 (1954).

[2] Camac, McGuire, Platt, and Schulte, Phys. Rev. **88**, 134 (1952); McGuire, Camac, Halbert, and Platt, Phys. Rev. **95**, 625 (1954).

[3] Camac, McGuire, Platt, and Schulte, preceding paper [Phys. Rev. **99**, 897 (1955)].